Nonradiative lifetime measurements in time-domain photoacoustic spectroscopy of condensed phases

A. Mandelis and B.S.H. Royce
Materials Laboratory, Princeton University, Princeton, New Jersey 08544

(Received 28 June 1979; accepted for publication 27 August 1979)

A theoretical model is presented for the time-domain photoacoustic response of a condensed sample with a two-level optical-absorption band. The nonradiative lifetime of the excited state and the transfer function of the pressure transducer are included in the formalism. The limitations of the technique for nonradiative lifetime measurements are discussed and the experimental conditions necessary for optimum relaxation time determinations are evaluated. It is found that the limitations imposed by the modified gas thermal transport equations used in the model restrict it to relaxation times greater than $\sim 10^{-5}$ sec. This is of the same order as the limit imposed on experimental measurements by the transfer function of commercial microphones.

PACS numbers: 78.20. – e, 78.65. – s, 42.80. – f, 07.65. – b

I. INTRODUCTION

When light is absorbed by an electronic state in a solid or liquid, the system may return to its ground state by emitting light, by nonradiative paths in which the excess energy appears as heat in the sample, or by photochemical processes. The lifetime of the excited state is determined by the relative rates for these competitive deexcitation paths, and the effective lifetime tends to be dominated by the fastest relaxation. Photoacoustic spectroscopy (PAS) provides a probe for those deexcitation processes that result in the liberation of heat and is thus complementary to measurements of fluorescence and phosphorescence. In the time domain the delay of the photoacoustic response with respect to the optical stimulus can provide information about the effective lifetime of the excited state, and measurements of this type are therefore of interest, particularly on materials for which the fluorescence quantum efficiency is low. If the material under study is stable photochemically, the magnitudes of the radiative and nonradiative process will anticorrelate.

The relaxation times of radiationless processes have been studied using frequency-domain PAS techniques by Powell and co-workers.[1-3] They employed the relationship between the nonradiative relaxation time and the phase of the photoacoustic response used by Harshbarger and Robin[4] for gaseous samples. Mandelis *et al.*[5] have derived the corresponding relationships between the photoacoustic phase and the nonradiative relaxation time for condensed samples. They have shown that only in the limits of an optically and thermally thick specimen or an optically transparent thermally thick sample is the relaxation time simply related to the photoacoustic phase. For other conditions additional contributions to the phase arise from the wavelength-dependent optical-absorption depth in the sample.

A one-dimensional theoretical model of the time evolution of the photoacoustic response of a solid sample which includes finite relaxation times for the nonradiative processes has been employed by Aamodt and Murphy.[6] The application of this model to data analysis is difficult because no analytic closed-form expressions are available for the inversion of the complicated Laplace transforms involved. In an attempt to overcome this difficulty Mandelis and Royce[7] employed a simplified form of the transport equations in the gas of the photoacoustic cell and derived an explicit closed-form expression for the time-domain response following excitation of a system with instantaneous nonradiative deexcitation processes by a single optical radiation pulse. For photoacoustic cell dimensions typical of experimental situations this simplified theory gave results in agreement with the more complete model for times longer than $\sim 10^{-5}$ sec, an acoustic transit time for the cell. Neither of these time domain papers took into account the transfer function of the pressure measuring transducer.

This paper is concerned with the extension of the theory of Ref. 7 to include the finite relaxation time τ of the radiationless deexcitation processes in a condensed sample and the transfer function of the pressure measuring transducer. The model presented allows analytical closed-form inversion of the Laplace transforms for the temperature and pressure in the cell and provides an algebraic expression for the time development of the relaxation-time-dependent photoacoustic signal. Linear control theory methods are then employed to evaluate the modifications to this signal introduced by the microphone-preamplifier transducer, and it is found that an additional signal time delay results due to the high-frequency rolloff of the microphone response. For commercially available condenser microphones this factor would restrict the PAS technique to the measurement of lifetimes longer than $\sim 10^{-5}$ sec. This limit is approximately the same as that imposed by the assumptions made in the evaluation of the cell pressure.

II. THEORY

A. PAS response including a nonradiative relaxation time

The one-dimensional geometry of the PAS system under consideration is shown in Fig. 1 and is essentially the same as that employed by Aamodt and Murphy.[6] The sample(s), of thickness l, contains a two-level optical-absorption band which has an excited-state lifetime τ and is associated with a wavelength-dependent optical-absorption coefficient β. The system is

 0021-8979/80/010610-06$01.10

stimulated by a light pulse in the form of a Heavyside function of duration τ_p and irradiance I_0. Following light absorption, the sample relaxes nonradiatively with an efficiency η. Under these conditions the sample experiences a spatially dependent head flux that is the time-domain equivalent of that given by Eq. (1) of Ref. 7 and which has the form:

$$\dot{H}(x,t) = (\beta I_0 \eta)\exp(\beta x)\begin{cases}[1-\exp(-t/\tau)], & 0\leqslant t\leqslant\tau_p,\\ [\exp(\tau_p/\tau)-1]\exp(-t/\tau), & \tau\geqslant\tau_p,\end{cases} \tag{1}$$

where $-l\leqslant x\leqslant 0$.

Following the procedure of Ref. 7, four coupled heat-diffusion equations can be written with only that for the solid containing the distributed heat source since the other regions of the cell are assumed to be optically transparent. The transport equation for the gas does not include terms due to the finite sound velocity, and this is equivalent to assuming that the gas pressure is uniform throughout the cell, whereas the temperature distribution has a spatial as well as a time dependence. The four coupled transport equations may be solved simultaneously using Laplace transform techniques with the boundary conditions of heat flux and temperature continuity at the interfaces of the regions of the cell. In this way the Laplace transform of the temperature in the gas, $\hat{T}(x,s)$, may be obtained and, by integration over the cell volume, an expression for the Laplace transform of the average pressure change in the gas can be derived. This has the form:

$$\Delta\hat{p}(s;\tau) = \Delta\hat{p}(s;0) - \left(\frac{\eta\beta I_0 p_0[1-\exp(-s\tau_p)]}{K_s L a_g T_0 (s+\tau^{-1})(\beta^2-a_s^2)}\right)[\cosh(a_g L)-1+D\sinh(a_g L)]$$
$$\times\left(\frac{(r-1)(b+1)\exp(a_s l)-(r+1)(b-1)\exp(-a_s l)+2(b-r)\exp(-\beta l)}{(b+1)[(1+gD)S+(D+g)C]\exp(a_s l)-(b-1)[(gD-1)S+(g-D)C]\exp(-a_s l)}\right), \tag{2}$$

where $\Delta\hat{p}(s;0)$ is the Laplace transform of the pressure response expected for a sample with instantaneous relaxations and is given by Eq. (12) of Ref. 7. The other symbols also have the same meanings as in that paper.

Equation (2) may be explicitly inverted in the limit of a thermally thick solid for which the sample thickness l is greater than the time-dependent thermal diffusion depth $\mu_s(t)$ for all times of interest and also for a thermally thin solid for which $l<\mu_s(t)$. The average pressure in the cell is then given by:

$$\langle p_g(t;\tau,\chi)\rangle = \langle p_g(t;0,\chi)\rangle - \left[(\alpha_s\beta\eta I_0 p_0\sqrt{\alpha_g})/T_0 L K_s\right]\left\{J[0,t;\tau,\chi]+2\sum_{n=1}^{\infty}(-1)^n J\left[\left(nL/\sqrt{\alpha_g}\right),t;\tau,\chi\right]\right\},$$
$$t\leqslant\tau_p \tag{3}$$

$$\langle p_g[(t>\tau_p);\tau]\rangle = \langle p_g[(t<\tau_p);\tau]\rangle_{t=t} - \langle p_g[(t<\tau_p);\tau]\rangle_{t=(t-\tau_p)}, \qquad t\geqslant\tau_p,$$

where $\langle p(t;0,\chi)\rangle$ is the cell pressure if the nonradiative relaxations are instantaneous and is given by Eq. (17) in Ref. 7. The quantity χ is a characteristic time ($\equiv\tau_\beta$ or τ_l in the thermally thick and thermally thin limits, respectively) that is also defined in Ref. 7. J is defined in the Appendix.

Figure 2 shows the form of the heat input and the time-dependent photoacoustic response for an optically opaque thermally thick sample obtained by numerical evaluation of Eqs. (1) and (3). The effect of the nonradiative relaxation time on the pressure signal appears as a time delay. $\dot{H}(t;\tau)$ is shown for the case where the relaxation time $\tau(=10^{-4}\text{ sec})$ is long compared to the pulse duration τ_p $(=5.5\times10^{-6}$ sec). Under these circumstances the excited-state population continues to build up for the duration of the pulse, and $\dot{H}(t;\tau)$ therefore exhibits its maximum value at the end of the pulse. When the stimulus is removed the excited-state population decreases with its characteristic relaxation time τ and the heat input to the solid exhibits a parallel decrease. Throughout this period the pressure in the gas is increasing due to heat transfer to it from the solid. The pressure response has an inflection point at $t=\tau$ provided τ is short compared to a thermal transit time of the cell but long compared to τ_p. These limitations restrict measurements of τ to the approximate range: $10^{-5}\leqslant\tau\leqslant0.1$ sec. By $t\simeq10\tau$ the excited-state population is depleted and no more heat is supplied to the solid. The surface temperature of the solid has not yet decayed to T_0 and some heat is still being supplied to the gas. At longer times heat transfer processes to the cell window reduce the gas pressure to its preexcitation value. For very long relaxation times the interplay between energy transfer to the gas from the photoexcited solid and energy loss to the window determines the form of the pressure response. This is illustrated in Fig. 2 by the $\tau=10^{-3}$-sec curve which does not reach the same maximum value of the pressure despite the fact that the total energy in the pulse was the same as for the other curves. This effect is even more marked for longer relaxation times or shorter thermal transit times.

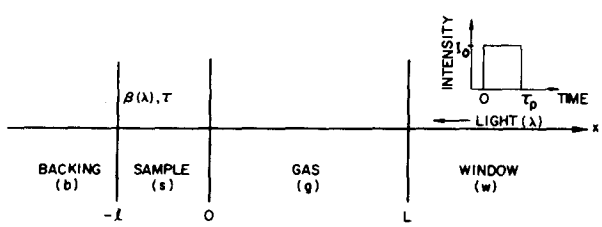

FIG. 1. Schematic diagram of the one-dimensional cell geometry.

The case presented in Fig. 2 is the only one for which the τ dependence of the pressure response is clearly resolvable. In the optically and thermally thin limit the pressure curves corresponding to different values of τ are distinct but there is no clear way of extracting lifetime data from them without fitting the theoretical expression to the complete pressure curve.

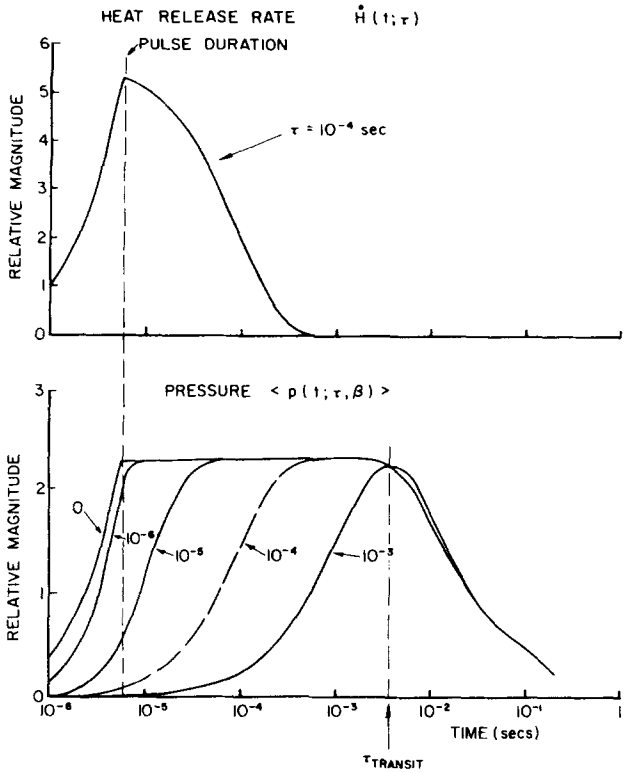

FIG. 2. Heat release rate to solid and cell pressure for various nonradiative relaxation times.

B. Effect due to the microphone transfer function

Previous papers on time-domain photoacoustic spectroscopy have only been concerned with the computed cell pressure rather than the output of a pressure-measuring device, the experimentally determined quantity. It is to be expected that the frequency response of the pressure transducer will impose a limit on relaxation time measurements. In this section the influence of the transducer's transfer function on the measured response is considered.

A mechanical model of the microphone was employed, the transducer being simulated by a spring-mass-damper system. The system is considered to be excited by an arbitrary force $F(t)$ produced by the time-dependent cell pressure acting over the area of the microphone diaphragm A_0, so that $F(t) = A_0 \Delta p(t)$. Under these conditions the differential equation describing the diaphragm motion in terms of the average coordinate z for the lowest-order mode is given by[8]:

$$m\ddot{z}(t) + \delta z(t) + K_m z(t) = F(t) = A_0 \Delta p(t), \quad (4)$$

where m is the mass of the diaphragm, δ is a damping coefficient, and K_m is the spring constant. The Laplace transform of the displacement may be obtained from Eq. (4) and has the form:

$$\hat{z}(s) = [(A_0/m)\Delta\hat{p}(s)]\,(s^2 + 2\zeta\omega_m s + \omega_m^2)^{-1}, \quad (5)$$

where $\omega_m \equiv (K_m/m)^{1/2}$ is the undamped natural angular frequency, $\zeta \equiv (\delta/2m\omega_m) = (\delta/\delta_{cr})$ is the damping factor, and $\Delta\hat{p}(s)$ is the Laplace transform of $\Delta p(t)$.

The simplified equivalent circuit of a condenser microphone and preamplifier is shown in Fig. 3.[9] The output voltage resulting from the displacement $z(t)$ which gives rise to a capacitance change $\Delta C(t)$ can be expressed in terms of its Laplace transform as:

$$\hat{V}(s) = E\left(\frac{\tau_{RC}s}{1+\tau_{RC}s}\right)\frac{\hat{z}(s)}{d}, \quad (6)$$

where d is the equilibrium distance between the diaphragm and the charge plate, τ_{RC} is the time constant of the equivalent circuit, and E is the polarization voltage. Equations (5) and (6) are combined to give the transfer function $Z(s)$ of the system,

$$Z(s) \equiv \frac{\hat{V}(s)}{\Delta\hat{p}(s)} = \left(\frac{Gs}{s^3 + a_2 s^2 + a_1 s + a_0}\right)\ \frac{\text{V}}{\text{Pa}}, \quad (7)$$

where $a_0 \equiv (\omega_m^2/\tau_{RC})$, $a_1 \equiv (\omega_m^2 + 2\zeta\omega_m/\tau_{RC})$, $a_2 \equiv (2\zeta\omega_m + 1/\tau_{RC})$, and G is a scaling parameter that matches the computed and experimental amplitudes.

The parameters in Eq. (7) can be determined by fitting to the published frequency response data of the transducer with s replaced by $i\omega$. This procedure was followed for the $\frac{1}{8}$-in. B&K condenser microphone Type 4138, chosen because of its flat high-frequency response. The best fit to the published frequency response data was found for $\tau_{RC} = 0.03$ sec, $\zeta = 0.7$, $\omega_m = 1.25\times10^6$ cycles/sec, and $G = 1.58\times10^9$ V Pa^{-1}sec^{-2}. Using these parameters it was found possible to match experimental square-wave response data given by the manufacturer. The fit to the frequency response curve is relatively insensitive to the values of ω_m and G, but the high frequency region is sensitive to the choice of ζ and the low-frequency rolloff to the choice of τ_{RC}. The values given above are such that the a_i satisfy the stability criteria[10] required of a third-order system, viz:

$$a_2 > 0 \quad \text{and} \quad a_1 a_2 - a_0 > 0. \quad (8)$$

Once the parameters of the microphone transfer function have been determined, the phase-variable theory of linear control systems[11] was employed to evaluate the time-domain response. The time response of the microphone-preamplifier combination is given in terms of the matrix differential equations:

$$\dot{\mathbf{x}}(t) = A\mathbf{x}(t) + B\mathbf{u}(t),$$
$$\mathbf{y}(t) = C\mathbf{x}(t), \quad (9)$$

where $\mathbf{u}(t)$ is the one-dimensional time-dependent input control function, $\mathbf{x}(t)$ is the three-dimensional state vector, $\mathbf{y}(t)$ is the one-dimensional output vector, A is the 3×3 system matrix, B is the 3×1 control matrix, and C is the 1×3 output matrix. These matrices are given by:

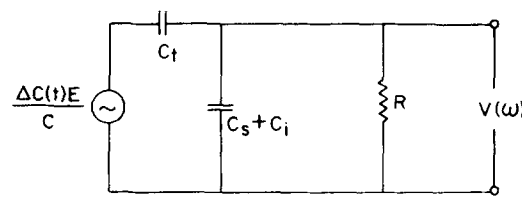

FIG. 3. Equivalent circuit of the capacitor microphone and preamplifier. C_f is the capacitance of microphone cartridge; C_s is the stray capacitance; C_i is the input capacitance of the preamplifier; $\Delta C(t)$ is the variation in capacitance due to sound pressure; $C = C_f + C_s + C_i$; R is the effective resistance of charging circuit and preamplifier.

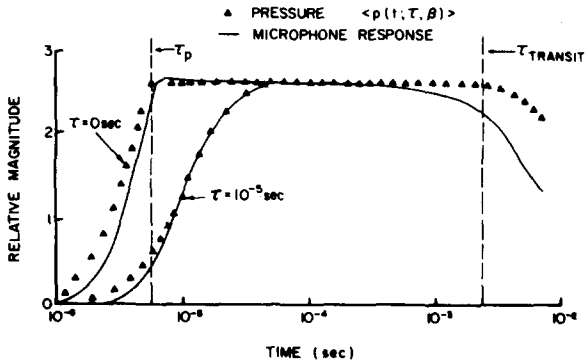

FIG. 4. Comparison between microphone response and pressure input for $\tau = 0$ and $\tau = 10^{-5}$ sec.

$$A = \begin{pmatrix} 0 & 1 & 0 \\ 0 & 0 & 1 \\ -a_0 & -a_1 & -a_2 \end{pmatrix},$$

$$B = \begin{pmatrix} 0 \\ 0 \\ G \end{pmatrix},$$

$$C = (0 \quad 1 \quad 0).$$

The formal solution for the system of Eq. (9) is as follows:

$$y(t) = x_2(t), \tag{10}$$

where $x_2(t)$ is the second component of the vector $\mathbf{x}(t)$ given by the matrix integral equation:

$$\mathbf{x}(t) = \exp(At)\mathbf{x}(0) + \int_0^t \exp[A(t-\lambda)]\mathbf{u}(\lambda)\, d\lambda. \tag{11}$$

The initial condition for the transducer at rest is $\mathbf{x}(0) = \mathbf{0}$. By use of the sample-data method[11] the continuous solution (11) can be transformed to a discrete-time solution:

$$\mathbf{x}[(n+1)T] = \exp(AT)\mathbf{x}(nT) + \left[\int_0^T \exp(A\lambda)B\, d\lambda\right]\mathbf{u}(nT), \tag{12}$$

where T is the sampling time interval.

Figure 4 shows a comparison between the pressure in the PAS cell and the microphone-preamplifier response using the parameters given above for the $\frac{1}{8}$-in. B&K microphone. Pressure curves for samples having $\tau = 0$ and 10^{-5} sec are given. It is seen that the high-frequency rolloff of the microphone appears as an early time delay in the transducer output for the $\tau = 0$ pressure stimulus. The overshoot at the beginning of the plateau is dependent upon the damping coefficient ζ. With this particular transducer, agreement between the pressure in the cell and the signal output at early times is seen to be satisfactory for $\tau \gtrsim 10^{-5}$ sec. The low-frequency preamplifier rolloff causes a decrease in the signal at long times since τ_{RC} is less than the thermal transit time of the PAS cell considered. This feature will interfere with thermal transit time measurements.

III. DISCUSSION

By introducing a simplified thermal transport equation for the gas phase of a pulse-stimulated photoacoustic system, it has been possible to obtain an analytical expression for the time-domain pressure development in the cell following excitation of a solid which has a finite nonradiative relaxation time. The results of this model are in good agreement with those obtained by Aamodt and Murphy[6] who employed a gas transport equation which included the finite velocity of sound. The models disagree at short times for which the more exact computation shows the presence of pressure steps associated with sound wave propagation within the cell. However, after about six such pressure steps, which are on the order of 10^{-4} times the final value of the cell pressure, the pressure increase predicted by the two models is in good agreement. Since these steps are small in magnitude and occur at early times in the pressure pulse development, their presence does not influence the determination of the excited-state relaxation time from the position of the inflection point in the $p(t)$ curve.

The most important limitation on the determination of τ is that provided by the transfer function of the pressure detector. The high-frequency rolloff of typical commercial devices introduces a time delay in the electrical output and probably restricts measurements of τ to times larger than 10^{-5} sec. This restriction is similar to that imposed by the uniform pressure approximation of the present model since the acoustic transit time of a photoacoustic cell of the dimensions normally employed for solid studies is on the order of 10–50 μs. It was found that the $\frac{1}{8}$-in. B&K microphone discussed above was capable of tracking the pressure pulses computed by Aamodt and Murphy[6]; however, the 1-in microphone (4145 B&K) had a poorer high-frequency response and tended to distort these pressure steps.

As indicated above, nonradiative lifetimes may also be measured using frequency-domain PAS techniques and determining the phase[5] of the system response with respect to the stimulating radiation. In order to make such measurements, data must be taken over a range of frequencies and the amplitude of the signal varies as ω^{-1} (or $\omega^{-3/2}$, depending upon the relative values of the optical-absorption depth and the thermal diffusion length in the material). Since high modulation frequencies are needed for the determination of short relaxation times, this decrease in signal amplitude imposes a restriction on the use of this method for the determination of such short relaxation times.

In the time domain the signal amplitude is not dependent upon the relaxation time provided energy loss to the cell windows is unimportant. This means that the technique is good for the measurement of short relaxation times. This behavior can be understood by examining the formalism leading to the PAS signal expressions in the two cases.

In the time domain, the expression for the signal involves an integration over the whole frequency spectrum. Energy is associated with each frequency interval and the distribution peaks in a different interval of the frequency space as t varies. The energy associated with each interval is $\Delta E_i = 2\pi I_0(\Delta\omega_i^{-1})$; however, the sum (integral) over all modes ω_i remains constant, and the signal is largely insensitive to locality changes in the energy distribution in ω space. Thus, even at early times there is a constant amount of energy averaged over all frequencies, which leads to a "short-

time signal strength" behavior. In the case of a fast relaxing optically opaque thermally thick sample, the signal level is the same at $t = 10^{-5}$ sec as it is at $t = 10^{-3}$ sec.[7] In the frequency domain, however, the formalism selects the modulation frequency ω_0 through the action of the δ function in the Fourier space integral for the pressure.[5] The signal, therefore, follows the same frequency dependence as its Fourier transform, and the one mode alloted all of the energy is that at ω_0 for which the energy varies as $E(\omega_0) = 2\pi I_0(\omega_0^{-1})$. Despite its advantage in short time signal strength, the time-domain technique is still limited by the finite velocity of sound and the occurrence of cell resonances. Both frequency- and time-domain methods that employ a gas as the information transfer medium will be restricted to measurements of nonradiative lifetimes greater than about 10^{-5} sec; however, both the insensitivity of the signal magnitude to the relaxation time of the nonradiative processes and the availability of high-powered pulsed-laser sources make the time-domain technique attractive.

ACKNOWLEDGMENTS

Partial support by ARO Contract No. DAAG29-76C-0054 is gratefully acknowledged. The authors would like to thank G. Bienkowski for useful discussions during the course of the work and L. Sweet for providing the DYNAMO computer program used to evaluate the time-domain response of the microphone.

APPENDIX

a. The function $J[Y,t;\tau,\tau_\beta]$:

$$J[Y,\tau;\tau,\tau_\beta] \equiv \mathscr{L}^{-1}\exp(-Y\sqrt{s})/s(s+\tau^{-1})(\sqrt{s}+1/\sqrt{\tau_\beta}) = \tau\sqrt{\tau_\beta}\{\operatorname{erfc}(Y/2\sqrt{t})$$
$$-(T/\tau)\exp[(t/\tau_\beta)+Y/\sqrt{\tau_\beta}]\operatorname{erfc}[Y/2\sqrt{t}+\sqrt{t}/\tau_\beta]-\tfrac{1}{2}\exp(-Y^2/4t)$$
$$\times\{(T/\tau_\beta)[\operatorname{Re}\{\exp(Z^2)\operatorname{erfc}Z\}+\operatorname{Re}\{\exp[(Z^*)^2]\operatorname{erfc}(Z^*)\}]$$
$$-(T/\sqrt{\tau\tau_\beta})[\operatorname{Im}\{\exp(Z^2)\operatorname{erfc}Z\}-\operatorname{Im}\{\exp[(Z^*)^2]\operatorname{erfc}(Z^*)\}]\}\},$$

where

$$\begin{Bmatrix} Z \\ Z^* \end{Bmatrix} = Y/2\sqrt{t} \pm i\sqrt{t/\tau}, \qquad T^{-1} \equiv \tau^{-1}+\tau_\beta^{-1}.$$

b. Computational aids for the evaluation of J. Error function of a complex argument, polar coordinate representation: By definition

$$\operatorname{erf}Z = 2/\sqrt{\pi}\int_0^Z \exp(-x^2)\,dx, \tag{A1}$$

where $Z = |Z|\exp(i\theta)$ in polar coordinates.

(i) In the sectors $-\frac{1}{4}\pi \leqslant \theta \leqslant \frac{1}{4}\pi$ and $\frac{3}{4}\pi \leqslant \theta \leqslant \frac{5}{4}\pi$, erf$Z$ converges and can be computed from consideration of the function

$$F(Z) = \int_0^Z \exp(x^2)\,dx \tag{A2}$$

by setting[12]

$$\operatorname{erf}Z = -2i/\sqrt{\pi}\,F(iZ). \tag{A3}$$

Then,

$$\operatorname{erfc}Z \equiv (1-\operatorname{erf}Z) = 1+2i/\sqrt{\pi}\,F(iZ). \tag{A4}$$

Defining $\operatorname{erfc}Z = \operatorname{Re}(\operatorname{erfc}Z) + i\operatorname{Im}(\operatorname{erfc}Z)$, taking real and imaginary parts of Eq. (A4), and using Ref. 12 gives,

$$\operatorname{Re}(\operatorname{erfc}Z) = \begin{cases} 1-2/\sqrt{\pi}\displaystyle\sum_{n=0}^{\infty}(-1)^n\frac{|Z|^{2n+1}\cos[(2n+1)\theta]}{n!(2n+1)} & \text{(Taylor)} \\ 2/\sqrt{\pi}\exp(-|Z|^2\cos 2\theta)\displaystyle\sum_{n=0}^{\infty}(-1)^n\frac{(2n-1)!!\cos[|Z|^2\sin 2\theta+(2n+1)\theta]}{2^{n+1}|Z|^{2n+1}} & \text{(Asymptotic)} \end{cases} \tag{A5}$$

$$\operatorname{Im}(\operatorname{erfc}Z) = \begin{cases} -2/\sqrt{\pi}\displaystyle\sum_{n=0}^{\infty}(-1)^n\frac{|Z|^{2n+1}\sin[(2n+1)\theta]}{n!(2n+1)} & \text{(Taylor)} \\ -2/\sqrt{\pi}\exp(-|Z|^2\cos 2\theta)\displaystyle\sum_{n=0}^{\infty}(-1)^n\frac{(2n-1)!!\sin[|Z|^2\sin 2\theta+(2n+1)\theta]}{2^{n+1}|Z|^{2n+1}} & \text{(Asymptotic)} \end{cases} \tag{A6}$$

$\frac{1}{4}\pi \leqslant \theta \leqslant \frac{1}{4}\pi, \quad \frac{3}{4}\pi \leqslant \theta \leqslant \frac{5}{4}\pi.$

(ii) In the sectors $\frac{1}{4}\pi \leqslant \frac{3}{4}\pi$ and $\frac{5}{4}\pi \leqslant \theta \leqslant \frac{7}{4}\pi$, the erfc$Z$ diverges. The inverse transform J can be evaluated by use of the function $\exp(Z^2)\operatorname{erfc}Z$, which converges in these sectors, and the Dawson function[13]:

$$D(Z) = \exp(-Z^2) \int_0^Z \exp(x^2)\, dx \tag{A7}$$

in the combination

$$W(Z) = \exp(-Z^2) + 2i/\sqrt{\pi}\, D(Z). \tag{A8}$$

Then,[14]

$$W(iZ) = \exp(Z^2)\,\mathrm{erfc}Z. \tag{A9}$$

Taking real and imaginary parts of Eq. (A9) and using Ref. 13 gives

$$\mathrm{Re}[\exp(Z^2)\,\mathrm{erfc}Z] = \begin{cases} \exp(|Z|^2\cos 2\theta)\cos(|Z|^2\sin 2\theta) - 2/\sqrt{\pi} \sum_{n=0}^{\infty} \dfrac{2^n |Z|^{2n+1}\cos[(2n+1)\theta]}{(2n+1)!!} & \text{(Taylor)} \\ 1/\sqrt{\pi} \sum_{n=0}^{\infty} (-1)^n \dfrac{(2n-1)!!\cos[(2n+1)\theta]}{2^n |Z|^{2n+1}} & \text{(Asymptotic),} \end{cases} \tag{A10}$$

$$\mathrm{Im}[\exp(Z^2)\,\mathrm{erfc}Z] = \begin{cases} \exp(|Z|^2\cos 2\theta)\sin(|Z|^2\sin 2\theta) - 2/\sqrt{\pi} \sum_{n=0}^{\infty} \dfrac{2^n |Z|^{2n+1}\sin[(2n+1)\theta]}{(2n+1)!!} & \text{(Taylor)} \\ -1/\sqrt{\pi} \sum_{n=0}^{\infty} (-1)^n \dfrac{(2n-1)!!\sin[(2n+1)\theta]}{2^n |Z|^{2n+1}} & \text{(Asymptotic),} \end{cases} \tag{A11}$$

$\frac{1}{4}\pi \leqslant \theta \leqslant \frac{3}{4}\pi, \quad \frac{5}{4}\pi \leqslant \theta \leqslant \frac{7}{4}\pi.$

Computationally, the point $|Z| = 3.9$ was found to be a good transition point from the Taylor to the asymptotic expansions, even though the exact number varies slightly for different θ's throughout the complex plane.

c. *Nontrivial integrals appearing during the inversion of the Laplace transform of J* (Ref. 15).

$$\int_0^t (dx/\sqrt{\pi x}) \exp(x/\tau) = -\sqrt{\tau}\,\mathrm{Im}[\mathrm{erfc}(i\sqrt{t/\tau})]; \tag{A12}$$

$$\int_0^t x^{-3/2} \exp[-(a^2/x) + b^2 x]\, dx = \mathrm{Re}\left((\sqrt{\pi}/2a)\left\{\exp(2iab)\,\mathrm{erfc}[(a/\sqrt{t}) + ib\sqrt{t}] + \exp(-2iab)\,\mathrm{erfc}[(a/\sqrt{t}) - ib\sqrt{t}]\right\}\right), \tag{A13}$$

$$\int_0^t x^{-1/2} \exp[-(a^2/x) + b^2 x]\, dx = \mathrm{Re}\left((i\sqrt{\pi}/2b)\left\{\exp(2iab)\,\mathrm{erfc}[(a/\sqrt{t}) + ib\sqrt{t}] - \exp(-2iab)\,\mathrm{erfc}[(a/\sqrt{t}) - ib\sqrt{t}]\right\}\right). \tag{A14}$$

[1] L.D. Merkle and R.C. Powell, Chem. Phys. Lett. **46**, 303 (1977).
[2] L.D. Merkle, R.C. Powell, and T.M. Wilson, J. Phys. C **11**, 3103 (1978).
[3] R.G. Peterson and R.C. Powell, Chem. Phys. Lett. **53**, 366 (1978).
[4] W.R. Harshbarger and M.B. Robin, Acc. Chem. Res. **6**, 329 (1973).
[5] A. Mandelis, Y.C. Teng, and B.S.H. Royce, J. Appl. Phys. (to be published).
[6] L.C. Aamodt and J.C. Murphy, J. Appl. Phys. **49**, 3036 (1978).
[7] A. Mandelis and B.S.H. Royce, J. Appl. Phys. **50**, 4330 (1979).
[8] L.B. Kreuzer, in *Optoacoustic Spectroscopy and Detection*, edited by Y.H. Pao (Academic, New York, 1977).
[9] *Microphones and Microphone Preamplifiers* (Brüel and Kjaer, 1976).
[10] C.C. Chen and I.J. Haas, *Elements of Control Systems Analysis* (Prentice Hall, Englewood Cliffs, N.J., 1967).
[11] D.G. Schultz and J.L. Melsa, *State Functions and Linear Control Systems* (McGraw-Hill, New York, 1967).
[12] K.A. Karpov, *Tables of the Functions* $F(Z) = \int_0^Z \exp(x^2)\, dx$ *in the Complex Domain*, translated by D.E. Brown (McMillan, New York, 1964).
[13] V.N. Faddeeva and N.M.. Tarentev, *Tables of Values of the Function* $W(Z)$ *for a Complex Argument* (Gosudarstv. Izdat. Tehn. Teor. Lit., Moscow, 1954).
[14] K.A. Karpov, *Tables of the Function* $W(Z) = \exp(-x^2)\int_0^Z \exp(x^2)\, dx$ *in the Complex Domain*, translated by D.E. Brown (Mcmillan, New York, 1965).
[15] The procedure followed in evaluating these integrals was similar to a method given by W. Horenstein, Quart. Appl. Math. **3**, 183 (1945).